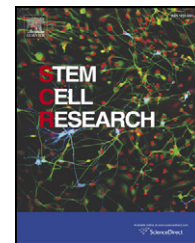Available online at www.sciencedirect.com

SciVerse ScienceDirect

www.elsevier.com/locate/scr

Inhibition of DNA methyltransferases and histone deacetylases induces astrocytic differentiation of neural progenitors

Anirban Majumder [a], Sujoy K. Dhara [b], Raymond Swetenburg [a], Miloni Mithani [a], Kaixiang Cao [c, d], Magdalena Medrzycki [c, d], Yuhong Fan [c, d], Steven L. Stice [a,*]

[a] Regenerative Bioscience Center, University of Georgia, 425 River Rd, Athens, GA 30602, USA
[b] Division of Veterinary Biotechnology, Indian Veterinary Research Institute, Izatnagar, Bareilly, UP 243 122, India
[c] School of Biology, Georgia Institute of Technology, 315 Ferst Dr. NW, Atlanta, GA 30332, USA
[d] Petit Institute for Bioengineering and Bioscience, USA

Abstract   Understanding how to specify rapid differentiation of human neural progenitor towards enriched non-transformed human astrocyte progenitors will provide a critical cell source to further our understanding of how astrocytes play a pivotal role in neural function and development. Human neural progenitors derived from pluripotent embryonic stem cells and propagated in adherent serum-free cultures provide a fate restricted renewable source for quick production of neural cells; however, such cells are highly refractive to astrocytogenesis and show a strong neurogenic bias, similar to neural progenitors from the early embryonic central nervous system (CNS). We found that several astrocytic genes are hypermethylated in such progenitors potentially preventing generation of astrocytes and leading to the proneuronal fate of these progenitors. However, epigenetic modification by Azacytidine (Aza-C) and Trichostatin A (TSA), with concomitant signaling from BMP2 and LIF in neural progenitor cultures shifts this bias, leading to expression of astrocytic markers as early as 5 days of differentiation, with near complete suppression of neuronal differentiation. The resultant cells express major astrocytic markers, are amenable to co-culture with neurons, can be propagated as astrocyte progenitors and are cryopreservable. Although previous reports have generated astrocytes from pluripotent cells, the differentiation required extensive culture or selection based on cell surface antigens. The development of a label free and rapid differentiation process will expedite future derivation of astrocytes from various sources pluripotent cells including, but not limited to, human astrocytes associated with various neurological diseases.

Introduction

Astrocytes are crucial to multiple aspects of nerve function and surpass neurons in abundance in the human central nervous system. Understanding the biology of human astrocytes or their potential in therapy is, however, undermined by lack of a steady source of non-transformed human astrocytes. Most researchers depend on primary astrocytes from mouse, or on human astrocytes from limited sources such as fetal brains or gliomas. Both are of limited availability, are mixed populations and likely subject to variability due to source. Additionally, astrocytes from glioma origin have abnormalities

---

* Corresponding author. Fax: +1 706 583 0071.
 E-mail address: sstice@uga.edu (S.L. Stice).

related to cancer (Gonzalez-Gomez et al., 2003; Yan et al., 2009).

Although Human Embryonic (hES) and induced Pluripotent Stem (hiPS) cells are potential sources of unlimited quantities of astrocytes, suitable methods for quick and controlled differentiation of astrocytes from these cells are not available. When ES cells are differentiated as embryoid bodies (EB) in suspension culture, both neurons and astrocytes are produced within a largely uncontrolled mix of mature phenotypes. Also generation of a clean population may require months of culture, delaying and potentially hampering the utility of hES or hiPS as sources of astrocytes for applications where multiple new pluripotent cell lines from additional genotypes must be quickly differentiated to astrocytes (Krencik et al., 2011). The EB cultures display mixed phenotypes and the means of directing differentiation are by nature inefficient because the various differentiating cells are not uniformly exposed to chemical/growth factor cocktails. Enriching astrocytes from such cultures requires flow cytometric cell sorting (FACS) or microbead-based separation based upon phenotypic markers (Yuan et al., 2011). However, this method is limited since the cultures must be either mechanically or enzymatically dissociated into single cells, which induces contractility-mediated programmed cell death (Chen et al., 2010; Ohgushi et al., 2010). The ability to quickly and separately derive both neurons and astrocytes that share the same cell source and hence the same genetic background, combined with iPS technology, will open up the possibility of designing patient- or population-specific tissue, representative screening and therapeutic approaches.

Other than the spontaneous production of astrocytes from hES cells, specification of astrocytes in more directed differentiation approaches has been described (Krencik et al., 2011; Gupta et al., 2012). Although highly enriched astrocyte cultures are produced, the process takes as long as 3 months and involves culture as 3 dimensional aggregates of cells (Krencik et al., 2011). An alternative approach for quick derivation of astrocytes utilizes an intermediate fate restricted population: human neural progenitors (hNP) derived from ES/iPS cells. Adherent hNP cells differentiate readily to form neurons that express numerous mature neuronal markers (Young et al., 2011). However, astrocytogenesis from hNP cells, although faster than when starting with hES, is still a long term differentiation process (greater than 125 days) and produces mixed populations rich in neurons (Young et al., 2011). Despite the length of time required to derive astrocytes from hNP cells there are several advantages to this process. First it eliminates the time and variability associated with ES/iPS cell culture and differentiation. Human NP cells derived from pluripotent cells are self-renewing, and can be expanded as required prior to further differentiation (Shin et al., 2006; Dhara et al., 2008), thus offering a renewable source of human astrocytes. Moreover differentiation in adherent monolayer cultures offers uniform access, increasing the ability to manipulate cells by chemical supplementation or manipulation by transfection, transduction, and RNAi approaches. To exploit these hNP cells as a consistent source of astrocytes, one has to be able to switch their proneuronal bias to a proastrocytic one.

Understanding of potential mechanisms involved in the initial inherent neuronal bias of cultures and then using small molecules to alter this bias towards astrocyte lineages will enable uniform and faster processes to generate astrocytes. Here we explore the epigenetic mechanism that maintains the proneuronal character of hNP cells and prevents generation of astrocytes. We also describe a method utilizing small molecules in a chemically defined, serum-free media to shift the bias of hNP cells from a proneuronal to a proastrocytic state, leading ultimately to the production of highly enriched astrocytic cultures within a very short time. These cells express prominent astrocytic markers in as little as 5 days of differentiation and generate highly enriched populations of astrocytes, making it possible to generate either neurons or astrocytes from the same progenitor source. Additionally, derivation and subsequent maintenance in the same basal media as neurons make these cells amenable to co-culture. The method also produces near complete suppression of neuronal fates, thus further improving the utility of the derived astrocytes.

Materials and methods

Cell culture and differentiation

Human neural progenitor (hNP) cell derivation from hES cells has been described previously (Dhara et al., 2008). hNP cells were propagated as adherent monolayer cultures in proliferation media (Neurobasal™, 1× B27, 1× Glutamax™, P/S, FGF2 10 ng/mL) as described (Shin et al., 2006). For neuronal differentiation FGF2 was removed from the propagation media (termed neuronal differentiation media). For astrocytic differentiation of hNP cells, neuronal differentiation media were supplemented with BMP2 (20 ng/mL) and combinations of Aza-C and TSA; Aza-C (500 nM), TSA (100 nM) and BMP2 (20 ng/mL) for 2 days, with one complete media change in between, followed by differentiation media supplemented with BMP2 but not with Aza-C or TSA. Cells were harvested prior to analysis at 5, 15 or 30 days of treatment or for cryopreservation at d6 or d10 of differentiation. For cryopreservation, cells were dissociated with Accutase™ and frozen in differentiation media containing 10% DMSO. Viability was assessed at 30 days in Aza-C and TSA treated cultures by trypan blue exclusion, and data was acquired using a Cellometer Auto T4® (Nexcelom Biosciences).

Immunocytochemistry, flow-cytometry and real time quantitative polymerase chain reaction

Immunocytochemistry and flow cytometry were performed as previously described (Majumder et al., 2012). hNP cells were differentiated in adherent culture as above and dissociated with Accutase™. For staining adherent cultures, cells were re-plated on Matrigel coated chamber slides 2 days prior to fixation in 4% PFA at d15 and d30. Antibodies used for immunocytochemistry of adherent cultures were S100B (1:200, DAKO), GFAP (1:500, Abcam), GLAST (1:200, Abcam), and ALDH1L1 (1:200, Abcam). For flow-cytometry dissociated cells were stained with S100B (1:200, DAKO), GFAP (1:100, Abcam) and GLAST (1:200, Abcam). Alexafluor (Invitrogen) dye conjugated secondary antibodies were used at 1:1000 for slides and 1:5000 for flow cytometry.

Total RNA was isolated using RNeasy Plus kit (Qiagen) and reverse transcribed using iScript cDNA kit. Real time qPCR was performed on an ABI Prism7900HT. Inventoried Taqman™

assays were used for all genes assayed. 3 replicates were run unless otherwise mentioned. Data was analyzed using SDS2.4 and DataAssist3.01 software (Applied Biosystems).

Bisulfite sequencing analysis

We compared methylation in hNP cells with that in populations differentiated in neuronal differentiation media (UT), differentiation media with BMP2 (BMP2), with BMP2, Aza-C 500 nM, TSA 10 nM (BMP2, Aza-C, TSA 10) or with BMP2, Aza-C 500 nM and TSA 20 nM (BMP2, Aza-C, TSA 20).

Genomic DNA was extracted, treated with the Bisulfite Conversion Kit (CpG Genome) and used for PCR as previously described (Zhang et al., 2012). The primer sequences are specific for the converted DNA sequence of the analyzed regions and are available upon request. PCR products were subsequently cloned using the TOPO TA cloning kit (Invitrogen), and colonies were picked and plasmid DNA from each clone was prepared. DNA was sequenced and analyzed with BiQ analyzer (Bock et al., 2005).

Quantitative chromatin immunoprecipitation (qChIP)

ChIP assays were performed as described previously (Zhang et al., 2012). Briefly, chromatin was crosslinked with formaldehyde and sheared by sonication. 20 μL of Dynabeads Protein G (Invitrogen) was incubated with 2 μg of antibody for 7 h at 4 °C, washed prior to incubation with 40 μg of soluble chromatin overnight at 4 °C. Dynabeads were subsequently washed and protein/DNA complexes were eluted in Elution Buffer (50 mM Tris−Cl pH 8.0, 10 mM EDTA pH 8.0, 1% SDS) by incubation at 65 °C for 15 min. Protein/ DNA complex was reverse cross-linked by incubation overnight at 65 °C. DNA was purified with a Qiagen DNA Isolation column (Qiagen), and quantified by real-time PCR for specific DNA fragments using the iQ SYBR Green Supermix (BioRad) and a MyIQ Real-Time PCR Detection System (BioRad). The values from ChIP with control antibody (IgG) were typically less than 5% of the ChIP values with the antibodies against histone modifications. The following antibodies were used: anti-H3K4me3 (Millipore 07-473), anti-H3K9Ac (Millipore 07-352); anti-H3 (Abcam 1791) and IgG (Millipore 12-370).

Statistical analysis

Student's t-test was used to compare data for this study at $p < 0.05$ level of significance. Analysis of variance (ANOVA) followed by Tukey's test was conducted either by using SAS 8.01 (SAS Institute, Cary, NC) or Daniel's XL toolbox (a free, open source add-in for Microsoft Excel) for all multiple comparison data.

Results

Differentiating hNP cells do not express astrocytic markers

Human NP cells (hNP) are derived from human embryonic stem cells and cultured in the presence of FGF2 (Dhara et

al., 2008). Upon withdrawal of FGF2 from hNP cells, cultures begin to differentiate towards neurons (Young et al., 2011). Since BMP2 and LIF are known pro-astrocytic growth factors (Nakashima et al., 1999), we determined whether hNP cells could form astrocytes when subjected to BMP2 and LIF after FGF2 withdrawal, using qPCR analysis for the proneuronal gene NEUROD1, the astrocyte progenitor gene CD44, and astrocytic markers S100B and GFAP.

Compared to undifferentiated hNP cells, cultures differentiated without BMP2 had significant ($p < 0.05$) up-regulation of NEUROD1 (over 100 fold), which was markedly curbed with BMP2 treatment (Fig. 1A). Expression of CD44 and S100B was reduced in differentiated cells ($p < 0.05$) compared to hNP cells at all three time points, irrespective of presence or absence of BMP2 treatment (Fig. 1B), although down regulation was more pronounced in BMP$^-$ cultures (Fig. 1C).

In long term BMP$^+$ cultures (60 days) we detected a few S100B$^+$ and GFAP$^+$ cells (Fig. 1D). These were mixed cultures, proneuronal and visually the proportion of astrocytes and neurons varied greatly between cultures. GFAP transcript could also be detected at this time point (~2 months of differentiation) in the BMP2$^+$ cultures.

Pro-astrocytic gene promoters are hypermethylated in hNP cells cultured in FGF2-containing medium

Since hypermethylation at promoter regions of astrocytic genes have previously been reported for neural progenitors isolated from the early mouse embryo (Fan et al., 2005; Takizawa et al., 2001), we characterized hNP cells for DNA methylation status of several relevant astrocytic and neuronal genes using an Illumina methylation array. Promoters of 3 prominent astrocytic genes, GFAP, S100B and AQP4, were hypermethylated in hNP cells (Fig. 1E), while the promoters for proneuronal genes NEUROD1, NEUROG1, NEUROG2 and NEUROG3 were hypomethylated. However, promoter of proneuronal gene NEUROD6 was found to be hypermethylated (Fig. 1F), consistent with previous reports that not all neural progenitors express NEUROD6. For example this gene by itself is dispensable for cortical development (Wu et al., 2005). Several other astrocytic gene transcripts that are usually expressed in astrocytes (Fatemi et al., 2008; Cahoy et al., 2008) were found hypomethylated (GDNF, BDNF, VIM, ALDH1L1 and CLU) (Fig. 1E). Hypermethylation of CD44, S100B, GFAP and AQO4 promoters was further confirmed by bisulfate sequencing (Fig. 5).

Concomitant treatment with Aza-Cytidine, Trichostatin-A and BMP2 promotes early differentiation of hNP cells to astrocytic fates

To modulate the epigenetic status of hNP cells, we treated them with DNA methyltransferase inhibitor Aza-Cytidine (Aza-C), and histone deacetylase inhibitor Trichostatin-A (TSA). Combinations of Aza-C, TSA and BMP2 (listed in Fig. 2A) were analyzed for effects on expression of the astrocyte progenitor marker CD44 and the astrocyte marker S100B. After 5 days of differentiation, cultures treated with BMP2 alone and Aza-C alone showed no significant up-regulation of either CD44 or S100B gene expression (Figs. 2A and B). In contrast, there was a ~50 fold up-regulation of
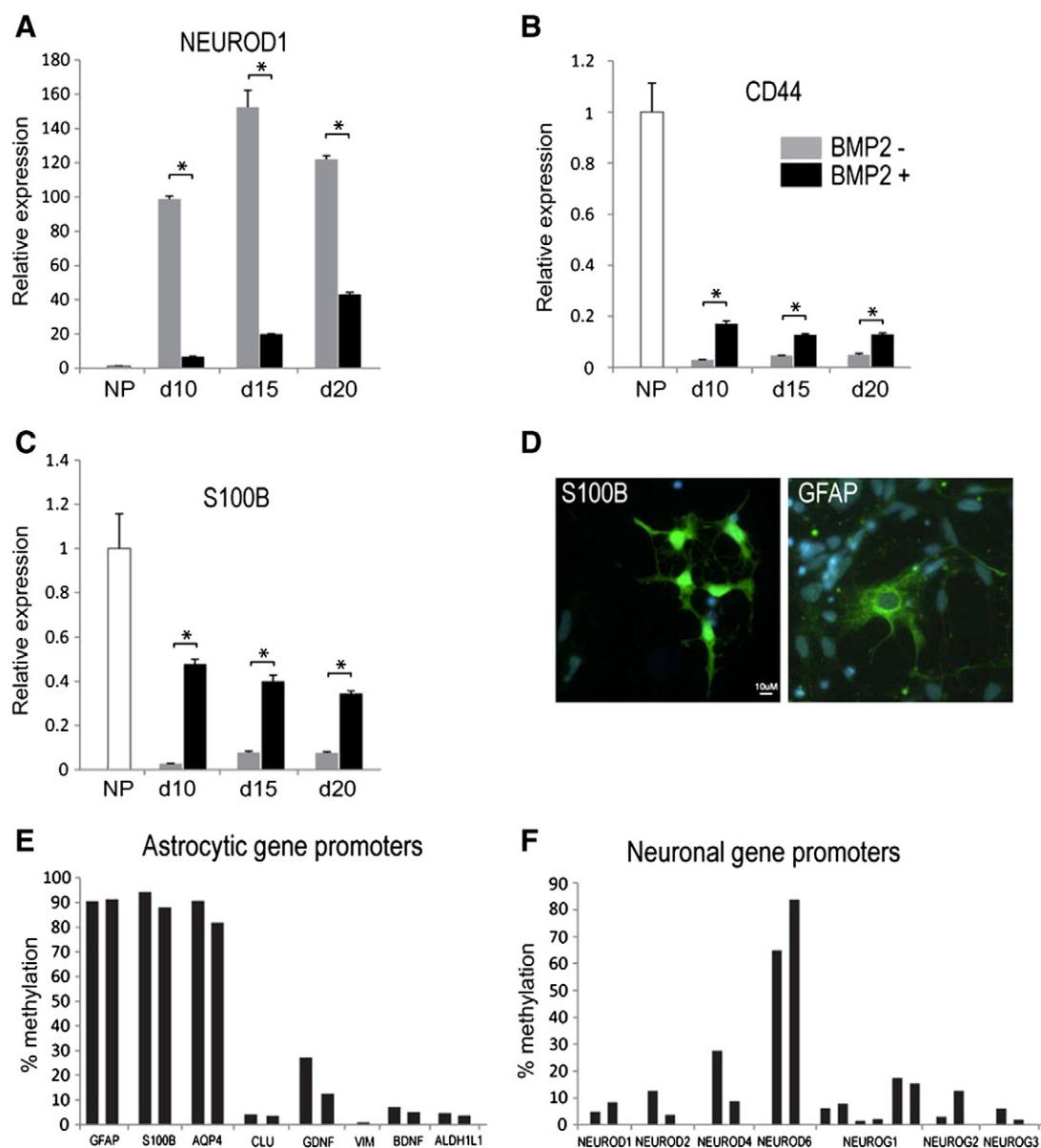
Figure 1 Effect of BMP2 on differentiation of human neural progenitors (hNP). Quantitative PCR detection of (A) neuronal marker NEUROD1, (B) astrocytic progenitor marker CD44 and (C) astrocytic marker S100B in differentiating hNP cells with or without a 5 day BMP2 treatment starting 5, 10 and 15 days post withdrawal of FGF2. Expression levels are calibrated to starting hNP population. Shown are the means ± SE for replicates (n = 3). Gray and black bars represent treatments without and with BMP2, respectively. (*) on bars indicates level of significance at p < 0.05. (D) Few S100B and GFAP immunoreactive cells are detected in culture differentiated for 60 days, including a 30 day BMP2 treatment. (E) Using an Illumina Methylation array, major pro-astrocytic gene promoters (GFAP, AQP4, and S100B) were found be hypermethylated (~80%), whereas (F), pro-neuronal genes (NEUROD1, NEUROD2, NEUROD4, NEUROG1, NEUROG2 and NEUROG3) were found to be hypo-methylated in hNP cells. Multiple loci for each gene were tested where probes were available and each bar represents one probe.

CD44 and greater than 50 fold up-regulation of S100B transcripts in cultures supplemented with BMP2 and Aza-C combined, compared to the starting hNP population. Treatment with Aza-C and TSA together, but with no concomitant BMP2 during the first 2 days, also led to >30 fold increase in CD44 expression and >150 fold increase in S100B gene expression (p < 0.05). However this treatment also produced the highest observed cell death amongst all the treatments. Concomitant treatment with BMP2 during the initial 2 day treatment with Aza-C and TSA maximized

expression (p < 0.05) of both CD44 (Fig. 2A) and S100B (Fig. 2B).

All Aza-C and TSA concentrations used above resulted in significant cell death; thus, we tested lower dose range responses for both compounds. No CD44 expression was detected in cells differentiated in neuronal differentiation media (referred to as untreated (UT) from here onwards) (Fig. 2C). With BMP2 alone (Aza-C 0 nM) expression level of CD44 was less than the starting hNP population. However, a dose dependent significant increase in CD44 expression was

observed between Aza-C 100 nM and 500 nM reaching >6 fold over hNP with Aza-C 500 nM (p < 0.05) (Fig. 2C). No further increase was seen with Aza-C at 1000 nM. A similar Aza-C dose dependency was evident for S100B, with no gene expression observed in UT control, and a 0, ~5 and ~10 fold increase over hNP at Aza-C concentrations of 0, 100 and 500 nM. At 1000 nM of Aza-C, expression of S100B was reduced (however, it was still 8 fold over hNP) (p < 0.05) (Fig. 2D). In the same experimental setup, a TSA dose dependent increase in expression of S100B but not CD44 transcripts was observed (p < 0.05) (Figs. 2F and E).

We further assessed expression of the astrocytic markers ALDH1L1, and GDNF, as well as the neuronal differentiation marker NeuroD1. ALDH1L1 transcripts were detected with all Aza-C containing conditions, with an increase at 500 μM over 100 μM. The highest response was noted at treatment with 500 nM Aza-C and 10 μM TSA (p < 0.05). No increase was seen in conditions containing TSA alone and no transcripts were detected in the untreated (UT) populations (Fig. 2G). GDNF expression was detected in all conditions containing Aza-C and no dose dependent effect of TSA was obvious. Similar to ALDH1L1, presence of 500 nM Aza-C and 10 nM TSA led to the highest expression levels of GDNF (p < 0.05) (Fig. 2H). Additionally, we tested expression of the astrocytic marker GFAP, but no GFAP transcripts were detected in the 5 day differentiated hNP cells irrespective of treatment (data not shown). NEUROD1 transcripts were detected in the starting hNP population. After differentiation, the untreated population had 60 fold higher expression of NEUROD1, while no transcripts were detected in any of the treated populations tested (Fig. 2I). Based on these data, the Aza-C 500 nM, TSA 10 or 20 nM and BMP2 20 ng/mL treatment was optimal for astrocytic differentiation of hNP cells and used in subsequent studies.

Morphological changes and expression of astrocyte markers after further differentiation

Human NP cells were treated with differentiation media containing Aza-C, TSA and BMP2 for two days and then maintained in differentiation media with BMP2 for a total of 15 days. Compared to untreated cultures, almost all cells in the treated populations were large, flat, and triangular or polygonal, and some had tapering extensions (Fig. 3A). Very few cells with neuronal morphologies were observed on the layer of astrocytes. In the control population, cells had small, refractive cell bodies and branched neurite extensions typical of neurons (Fig. 3B).

Immunocytochemistry data showed that a large fraction of cells in treated populations were positive for GFAP (Fig. 3C) and S100B (Fig. 3D) at d15. The GFAP immunoreactivity was weak and cytoplasmic while S100B was observed in both nucleus and cytoplasm (Fig. 3D). Untreated cells showed no immunoreactivity. Flow cytometry of d15 cultures indicated that the population was 20.9% ± 0.81 GFAP+ and 80.7% ± 0.83 S100B+ cells (Figs. 3C and D).

When the cultures were extended an additional 15 days (d30) in the same conditions, S100B+, GLAST+, CD44+ as well as ALDH1L1+ were detected by immunostaining. Most of these cells also co-stained weakly with GFAP (Figs. 3E–G). At both d15 and d30, GFAP and S100B negative cells were morphologically similar to the expressing cells. Approximately 58.44% ± 6.8 cells expressed S100B, and included strong (12% ± 3.7) as well as weakly (45.05 ± 3.04) immunoreactive cells. A very small fraction of cells showed very strong GFAP expression. Additionally a fraction of cells expressed CD44 and included both strong (9% ± 2.8) and weakly (28.6% ± 4.1) immunoreactive cells. In ALDH1L1+ and GFAP+ stained cells, the ALDH1L1 immunoreactivity was punctate and usually surrounding the nucleus (Fig. 3G). Similar ALDH1L1 staining pattern was obtained when human fetal derived astrocytes were stained with the same antibody (data not shown).

To further confirm the cellular identity of the cells in culture, we compared expression levels of several neuronal and astrocytic genes between treated and untreated cultures at d15 and d30 (Fig. 4). The astrocytic genes CD44, S100B, AQP4 and GJA1 were expressed at significantly higher levels (p < 0.05) in treated cultures at both day 15 and 30 compared to corresponding untreated controls. Although an uptrend was observed for BDNF in treated cultures at d15, a significant (p < 0.05) increase was observed only at d30. GFAP expression was detected at both d15 and d30, and d30 was significantly higher than d15. No GFAP transcripts were detected in either hNP or UT differentiation cultures (data not shown). Expression of SLC1A2, a glutamate transporter, was significantly higher for both treated and untreated populations at d30 compared to d15. The early neuronal marker NEUROD1 was detected in untreated controls at d15, with a reduction at d30, and was not detected in treated cultures at d30. Transcript levels of the mature neuronal marker MAP2 were highest in untreated cultures at d30, with significantly lower expression in the corresponding treated cultures (p < 0.05). Together there was a significant increase in astrocytic gene expression and decreased levels of neuronal gene expression in proastrocytic cultures. Azacytidine (Aza-C) and Trichostatin A (TSA) can

Figure 2 Gene expression in differentiating hNP cells to identify optimal treatments for astrocytic differentiation. Quantitative PCR is performed for astrocytic differentiation markers and relative expression of these markers is presented as bar diagrams (mean ± SE). Bar diagrams show average expression of (A) CD44 and (B) S100B in cells treated with combinations of FGF2 (10 ng/mL), Aza-C (1000 nM), TSA (50 nM) and BMP2 (20 ng/mL). In a separate culture, in the presence of an increasing Aza-C dosage, expressions of these markers [(C) CD44 and (D) S100B] were quantified. Data indicate that up to 500 nM of Aza-C is sufficient to differentiate hNP cells expressing CD44 and S100B. Here, NP and UT represent starting undifferentiated cells and neuronal differentiation, respectively. Therefore, in the next experiment, relative expressions of proastrocytic genes (E) CD44, (F) S100B, (G) ALDH1L1 and (H) GDNF were quantified for cultures treated with increasing concentrations of TSA against different levels of Aza-C and a constant level of BMP2. (I) Expression of NEUROD1 in untreated (UT) neuronal cultures relative to undifferentiated cells (NP). Transcripts were not detected in any of the remaining treatments tested. ANOVA followed by multiple comparisons using Tukey's test was performed. n = 3. Different superscripts on bars imply significant difference at p < 0.05 level.
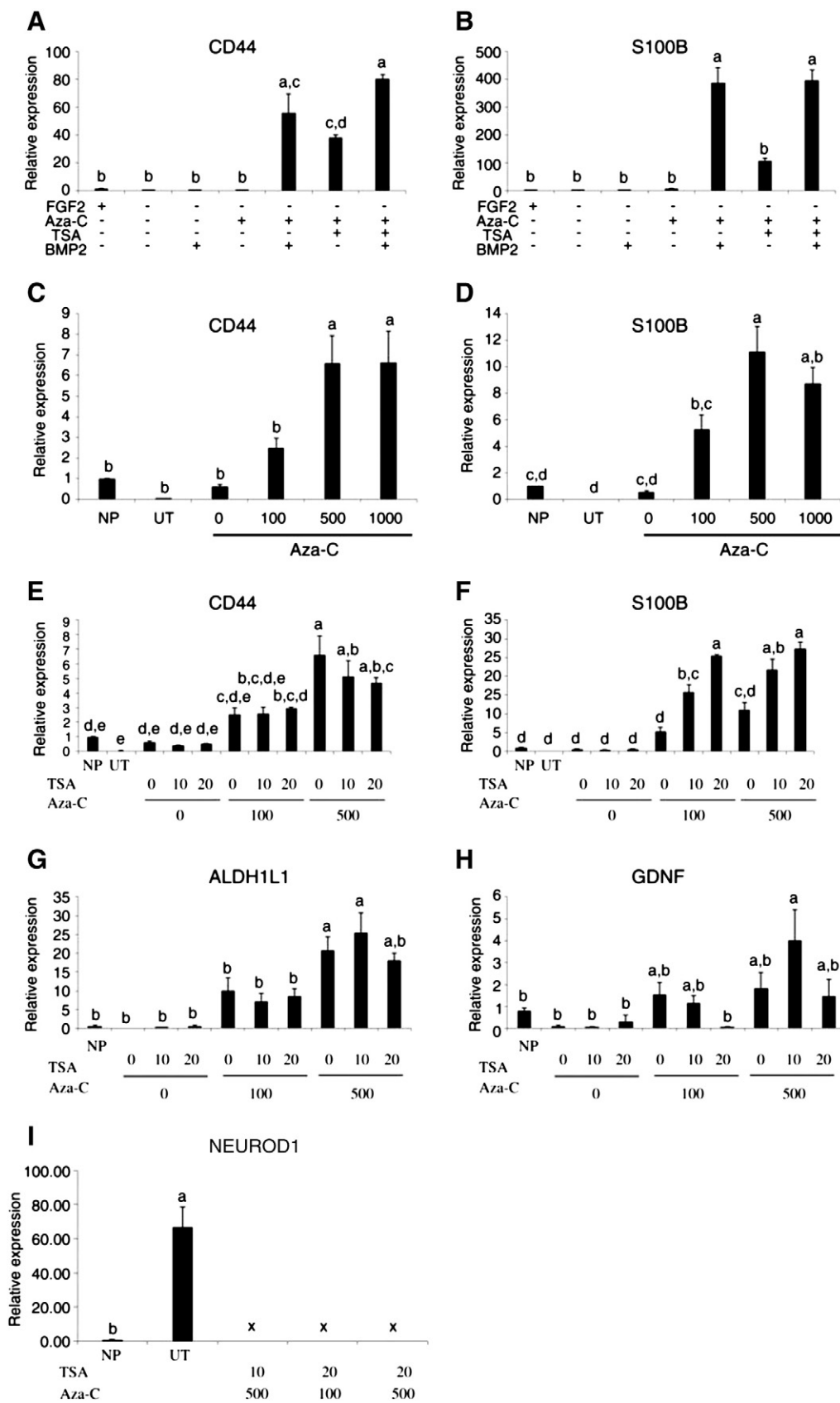
affect the long term viability of treated cells. Thus we conducted viability assays after 30 days of differentiation. Our results indicate a viability of 81% (±3.85), which is comparable to control neuronal cultures.

Dynamic epigenetic regulation of astrocytic genes during proastrocytic differentiation

To investigate the potential mechanisms by which our method regulates the expression of astrocytic genes, we analyzed the DNA methylation status of the promoter regions of astrocyte progenitor gene CD44 (Figs. 5A and C), and astrocyte genes S100B and GFAP (Figs. 5B and C). Bisulfite sequencing analysis showed that 40% of the CpG sites at the CD44 promoter region were methylated in cultured hNP cells with specific CpG sites being completely methylated (Figs. 5A and C). However, DNA methylation at the CD44 promoter was largely lost following withdrawal of FGF2 for 5 days (Untreated, UT) ($p < 0.0001$), and the promoter remained unmethylated in all treatments: BMP2 alone (BMP2) or BMP2 and Aza-C combined with TSA at two different concentrations (BMP2, Aza-C, TSA 10 nM or BMP2, Aza-C, TSA 20 nM) (Figs. 5A and C). In contrast to CD44, both GFAP and S100B were completely methylated in hNP cells. While removal of FGF2 and addition of BMP2 did not lead to significant changes in DNA methylation in these two genes, treatment with Aza-C and TSA caused significant increases in the percentage of unmethylated CpGs, with a larger effect on S100B than GFAP (Figs. 5B and C; $p < 0.01$ and $p \leq 0.0001$, respectively). These results demonstrate that treatment of Aza-C and TSA leads to reduced levels of DNA methylation at GFAP and S100B.

We next analyzed the status of two active histone marks, H3 lysine 9 acetylation (H3K9Ac) and H3 lysine 4 trimethylation (H3K4me3), at the promoters of CD44 and the astrocyte genes GFAP, S100B and AQP4 by quantitative chromatin immunoprecipitation (qChIP). As expected, H3K9Ac showed a dosage dependence on the concentration of TSA, an inhibitor of histone deacetylases (Fig. 6A, BMP2, Aza-C, TSA 10 nM vs BMP2, Aza-C, TSA 20 nM). The increases in H3K9 acetylation on proastrocytic genes correlate with increased levels of the active histone methylation mark, H3K4me3. H3K4me3 progressively increased with the addition of Aza-C and an increasing dose of TSA at astrocytic progenitor gene or astrocyte genes, but not at the house-keeping gene GAPDH (Fig. 6B). These results indicate the specific effects on the epigenetic regulation of astrocytic genes by concomitant treatment with Aza-C, TSA and BMP2.

Discussion

Human NP cells (hNP) differentiate readily to form neurons upon withdrawal of FGF2 from proliferation medium. By 15 days, a majority of the cells acquire neuronal morphologies and express a multitude of neuronal markers. However, even after long term differentiation (up to 125 days), there is a marked lack of astrocytic morphologies and marker expression (Young et al., 2011). Our study points to possible reasons for this neurogenic bias and provides a method for shifting this bias to produce an astrocytic population in a short period of time. To our knowledge, this is the first report describing the use of Aza-C and TSA to obtain astrocytes in such a short time

from human ES derived adherent NP cells. With the described treatments, in as little as 10–15 days, most, if not all cells in the population exhibit astrocytic morphologies, distinctly deviating from untreated cultures.

BMP2 inhibits neuronal specification but does not promote astrocytogenesis in human hNP cells

Synergism of BMP and LIF signaling is an established effector for astrocytic differentiation in primary cultures of rodent NP cells (Nakashima et al., 1999; Yanagisawa et al., 2001; Koblar et al., 1998). In a previous report on generation of astrocytes from human ESC, neural aggregates were dissociated and cultured for a month to get homogenous progenitors and another 55 days till they expressed BMP and LIF receptors. At this time the cells responded to BMP4 and LIF with astroglial specification (Gupta et al., 2012). However, our results indicate that hNP cells derived from hESC as adherent monolayers express LIF and BMP receptors but remain refractive to astroglial specification.

We have reported earlier that LIF signaling has a strong neurogenic effect during postmitotic differentiation of hNP cells (Majumder et al., 2012). Consistent with this, hNP cells differentiated with LIF but without BMP2 show a large increase in expression of NEUROD1 (Fig. 1A) and these cultures display a distinctly neuronal phenotype (by morphology). NEUROD1, a marker for early neuronal differentiation, promotes expression of Neurogenins that are known to inhibit astrocytogenesis and drive differentiation down the neuronal lineage (Sun et al., 2001). Further, our results here show that LIF and BMP2 signaling together, at least in the early phases of differentiation (up to 2 weeks), suppress neurogenesis, as reflected by significant reduction in NEUROD1 expression (Fig. 1A), but do not induce astroglial differentiation. Suppression of the preferred neurogenic pathway may, however, have a permissive effect on astrocytogenesis.

In both BMP2$^+$ and BMP2$^-$ differentiation, reduced expression of the astrocyte progenitor marker CD44 (Liu et al., 2004) and the astrocyte marker S100B is consistent with previously observed lack of astrocytic potential of these hNP cells (Young et al., 2011; Dhara et al., 2008). These data show that hNP cells are able to respond to BMP2 and that BMP2 is inhibitory to neuronal differentiation but not instructive in astrocytogenesis in early stages of differentiation.

When hNP cells were differentiated for a prolonged period (~2 months) in the presence of BMP2, a small fraction of cells expressed S100B and GFAP (Fig. 1D). It has been previously reported that, in neural progenitors cultured and expanded as aggregates, a small fraction of cells spontaneously express S100B at 30 days and GFAP expressing cells begin to appear at about 2 months (Krencik et al., 2011). This, however, is without addition of extrinsic BMP2. In contrast, the adherent hNP cells differentiated without BMP2 do not spontaneously differentiate to astroglial phenotypes when cultured up to 4 months (Young et al., 2011). Our results suggest that at least some cells in the differentiating population do acquire a proastrocytic BMP2 response with time. The fact that hNP cells are primarily neurogenic and do not respond to BMP2
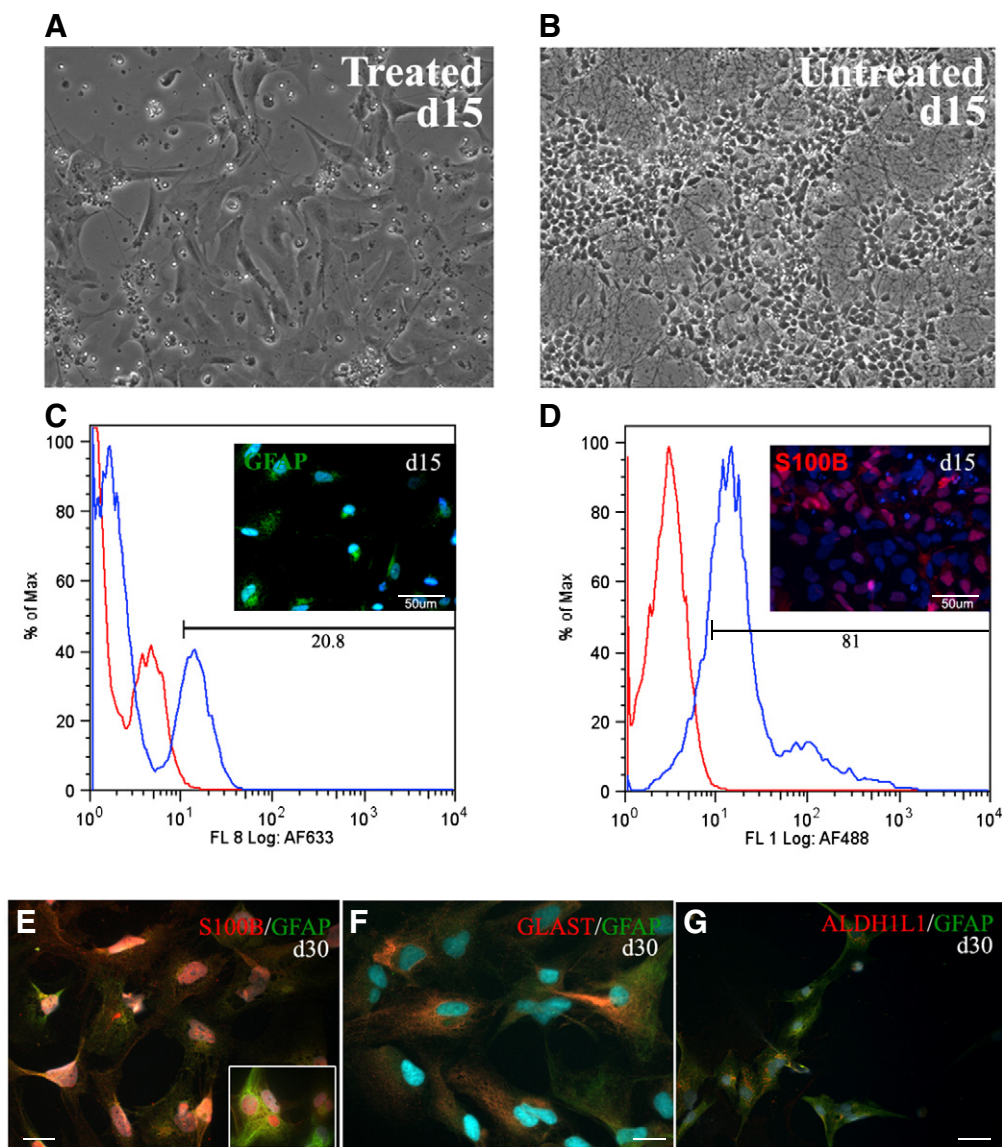
Figure 3 Morphology and gene expression after 15 and 30 days of differentiation of cells with astrocytic treatment. Bright field images of hNP cells differentiated (A) with or (B) without astrocytic treatment. A and B compare morphology of cultured cells in treated *vs.* untreated differentiation at 15 days. Treated and untreated cells were cryopreserved at d6 and subsequently thawed and cultured for an additional 9 days. Flow cytometry analysis to determine percent of GFAP[+] and S100B^{+} cells at d15 of differentiation. Data is presented as histograms for (C) GFAP and (D) S100B with corresponding immunoreactive cells in insets from a parallel culture. Immunocytochemistry detects expression of (E) GFAP with S100B (inset showing distinct staining for both markers), (F) GFAP with GLAST, and (G) GFAP with ALDH1L1 at d30 of differentiation.

and LIF signaling to produce astrocytes is reflective of rodent NP cells isolated from the early embryonic brain. These NP cells are not responsive to BMP2 and LIF until mid-gestation when they acquire astrocytic potential (Temple, 2001; Molne et al., 2000), and thus possibly represent early *in vivo* neuroepithilia.

Since BMP2 and LIF failed to generate astrocytes from hNP cells we examined the role of epigenetic regulation for glial differentiation. Changes in DNA methylation are critical for the switch from early neurogenic to late gliogenic potential of progenitor cells in the developing rodent brain (Fan et al., 2005; Wu et al., 2003; Shimozaki et

al., 2005). The inability of early rodent embryonic brain cells to produce astrocytes is attributed to promoter hypermethylation of prominent astrocytic genes (Takizawa et al., 2001), and the developmental shift in response is attributed to demethylation of these gene promoters during later stages of development (Hatada et al., 2008). The hypermethylation of GFAP, S100B and AQP4 that we detected in hNP cells, is correlative with the phenomenon described in the early mouse embryonic brain. Even after prolonged culture and passaging, the hNP cells remain proneuronal, with hypermethylated states maintained. Although not tested, we speculate that this is due to a lack
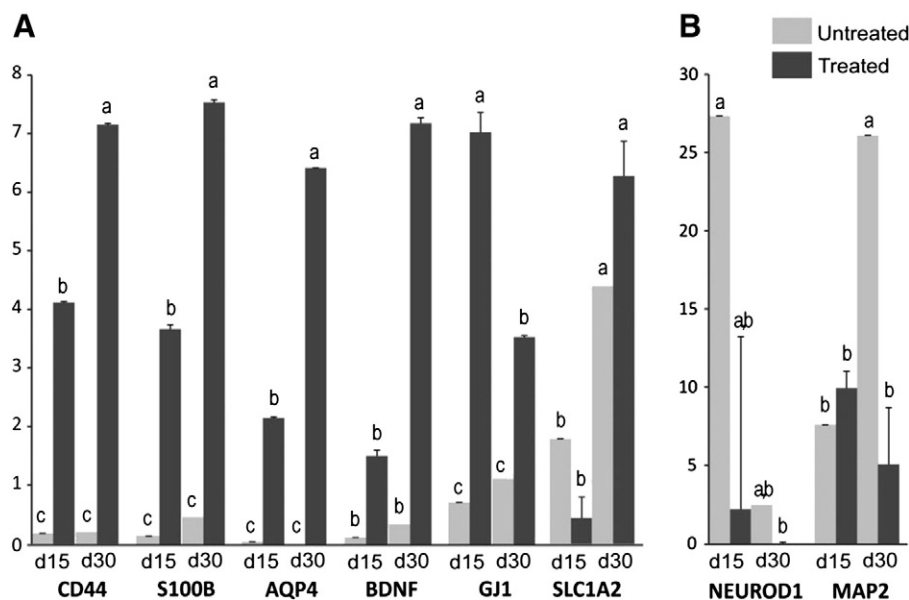
Figure 4 Astrocytic and neuronal gene expression analysis at 15 and 30 days of astrocytic and neuronal differentiation. Quantitative PCR was performed to detect both astrocytic and neuronal markers in hNP cells differentiated for 15 and 30 days. The mean (±SE) of replicates (n = 3) is presented as bar diagrams. ANOVA followed by Tukey's test for multiple comparisons was conducted. Panel (A) shows expression of astrocytic genes (CD44, S100B, AQP4, BDNF, GJ1, and SLC1A2) calibrated to undifferentiated hNP cells. All genes expressed significantly higher in amount at both day 15 and 30 of differentiation compared to untreated control. GJ1 had higher relative expression at day 15 whereas remaining genes had the highest expression at day 30 of differentiation. Panel (B) shows neuronal gene (NEUROD1 and MAP2) expression of untreated and treated populations. Differentiation promoted expression of neuronal markers in the untreated group which were significantly higher than the treated group. n = 3. Bars represent mean relative quantities within each gene and different superscripts within each gene imply significant differences ($p < 0.05$).

of adequate cell–cell signaling expected in the 3D environment of an embryoid body or in a developing embryo.

Combined exposure to Aza-C and TSA leads to early astrocytic differentiation

Azacytidine (Aza-C) is a DNA methyltransferase inhibitor that causes DNA demethylation (Juttermann et al., 1994; Santi et al., 1984). The demethylation of astroglial gene promoters enhances the competence of rodent neural progenitors to respond to astrogliogenic signals and cytokines such as BMP2, CNTF and LIF, enabling astrocytosis (Takizawa et al., 2001). Histone acetylation is another critical epigenetic controlling mechanism for neurogenesis (Mattson, 2003; Asano et al., 2009; Sanosaka et al., 2008) and has been implicated in astrocyte specification in the rodent (Freeman, 2010). Trichostatin-A (TSA) is a class I and II mammalian histone deacetylase (HDAC) inhibitor and can alter gene expression by interfering with the removal of acetyl groups from histones. The effects of TSA, however, depend to some extent on the target progenitor cells. In rodent embryonic neural stem cells undergoing *in vitro* differentiation, TSA promotes neuronal differentiation and appears to inhibit astrocytogenesis (Balasubramaniyan et al., 2006). However, the neural progenitor cells extracted from the adult hippocampal region of mouse differentiated into astrocytes upon HDAC inhibition, and addition of LIF and BMP (Gage et al., 1995; Chireux et al., 1996; Hersh and Shimojo, 2003). Given these progenitor-specific differences, it is necessary to specifically test its role in the context of the cell type of interest, that is, hES derived hNP cells.

Here we found that concomitant BMP2 and Aza-C treatment was needed for astrocytic differentiation of hNP cells (Figs. 2A and B). We showed that expression of both CD44 and S100B increases in a dose dependent manner for Aza-C, in a background of constant BMP2 and LIF, suggesting that Aza-C promoted both astrocytic progenitor fates (CD44) and maturation (S100B) (Figs. 2C and D). However, increasing the amounts of TSA in a background of constant Aza-C and BMP2 shows TSA dose dependence for expression of S100B (Fig. 2F), but not for CD44 (Fig. 2E), suggesting that TSA may be relevant to generation of the more mature phenotypes. ALDH1L1, which is expressed in rodent brain derived astrocytes (Anthony and Heintz, 2007; Fu et al., 2009), is expressed in treated hNP cells. ALDH1L1 expression depended more on Aza-C concentration than on TSA concentration (Fig. 2G). GDNF, another established marker of astrocytes, was expressed only in treated cells and not in the untreated cells (Fig. 2H), a further indication that these were proastrocytic treatments.

Multiple morphologies, including large flat triangular and polygonal cells, often with long tapering extensions and some with vacuolar structures seen in the treated hNP cell cultures (Figs. 3A and B), are similar to those described in detail for mouse astrocytes cultured *in vitro* (Matyash and Kettenmann, 2010). Astrocytic identity at this time is also confirmed by S100B and GFAP immunocytochemistry (Figs. 3C and D). During astroglial specification from hES derived neurospheres, S100B expression is observed in about 8% of cells at day 30 and GFAP expressing cells start to appear at about day 60, with changes in morphology in a corresponding fraction of cells (Krencik et al., 2011). In contrast, we observed S100B expression in a majority of cells within 15 days (Fig. 3F) along with GFAP
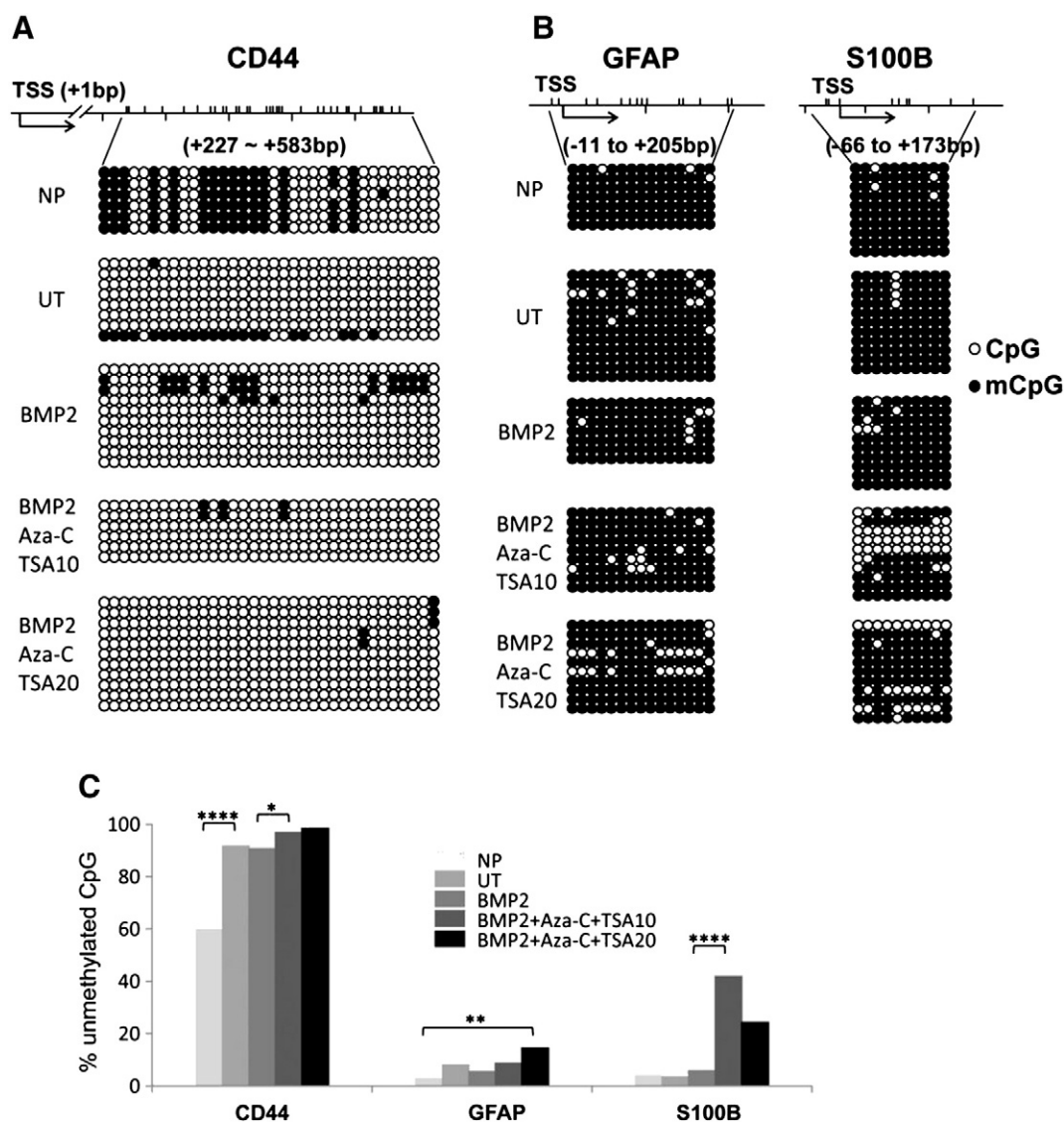
Figure 5 Changes in DNA methylation at astrocytic promoters following Aza-C and TSA treatment. Bisulfite sequencing analysis of DNA methylation status at promoters of (A) astrocyte progenitor gene CD44, and (B) the astrocyte genes S100B and GFAP. The position of CpG sites analyzed is indicated as vertical ticks on the line. TSS: transcription start site. Open circles: unmethylated CpG sites; closed circles: methylated CpG sites. (C) Percentage of unmethylated CpG sites. n = 3. Statistical analysis was performed using Fisher's exact test.*: $p < 0.05$, **: $p < 0.01$, ****: $p \leq 0.0001$.

expression in a smaller fraction. Appearance of an astroglial morphology throughout the treated cultures, and complete morphological divergence between the treated and untreated hNP populations further demonstrates the effectiveness of the treatment. After further differentiation/maintenance, at day 30, we still detect expression of both S100B and GFAP, and a major fraction of cells co-express both. The expression levels of S100B fall within a wide range. GFAP remains low in majority of the cells compared to fetal brain cell control and possibly indicate non-reactive astrocytes that do not often express GFAP at an immunohistochemically detectable level (Sofroniew and Vinters, 2010). The small and scattered clusters of strong GFAP positive cells are likely spontaneously reactivated astrocytes. ALDH1L1 and GLAST immunoreactivity further confirmed the astrocytic identity at this stage (Fig. 3). Additionally the presence of a CD44 immunoreactive fraction

suggests that astrocytic progenitors are still present at this stage.

Aza-C and TSA treatment promotes specific epigenetic changes at proastrocytic gene promoters

Removal of FGF2 resulted in a significant demethylation at the CD44 promoter region even in the absence of Aza-C treatment. This suggests that FGF2 was required for maintenance of DNA methylation and repression of CD44 expression. It is interesting to note that treatment with Aza-C and TSA caused nearly complete depletion of methylated CpG in the CD44 promoter in the population, suggesting that Aza-C and TSA treatment prevents DNA methylation and stabilizes an active state of CD44 promoter.
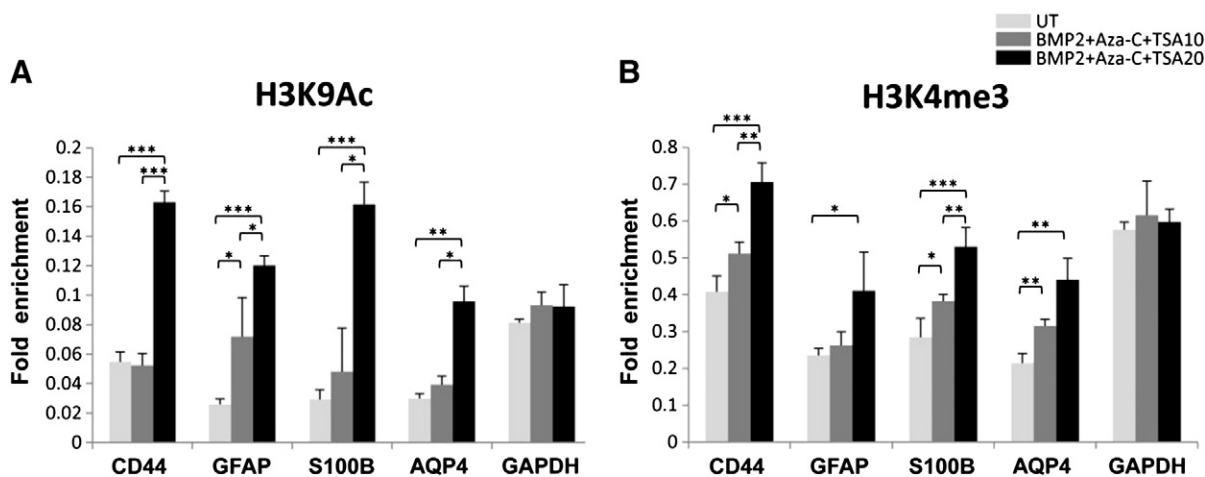
A

H3K9Ac

B

H3K4me3

Figure 6 Quantitative chromatin immunoprecipitation (qChIP) analysis of histone marks at astrocytic promoters following Aza-C and TSA treatment. The levels of (A) H3K9Ac and (B) H3K4me3 were analyzed by qChIP and normalized to input controls. Fold enrichment was represented as fold changes over that of histone H3. The dashed line indicates the highest signal level of control IgG qChIP. n = 3. Data are presented as mean ± SD. *: $p < 0.05$, **: $p < 0.01$, ***: $p < 0.001$.

Promoter regions of S100B and GFAP genes were stably repressed in hNP cells without any significant reduction in methylation by removal of FGF2 or by addition of BMP2 in culture. Here, we show that a higher dose of TSA leads to an increased level of H3K9Ac acetylation, supporting a role for TSA in inhibiting histone deacetylation. Additionally, the levels of the active mark H3K4me3 also increase at astrocyte genes, further suggesting an active state of these promoters. Interestingly, the impact of Aza-C and TSA on the epigenetic profiles of these astrocyte genes appears to be specific. These results suggest that Aza-C and TSA promote the transition of the promoters of these astrocytic genes from an inactive to active state, facilitating the rapid up-regulation of the gene expression under the *in vitro* conditions we developed here using small molecules.

Given our data, it is likely that overall astrocytic differentiation is governed by FGF2, BMP2 and LIF signaling in hNP cells pre-exposed to Aza-C and TSA (Fig. 7). FGF2, a mitogen, maintains undifferentiated progenitor cell state negatively regulating hNP cell differentiation. Once FGF2 is withdrawn, hNP cells readily become postmitotic neuronal cells. However, even in the presence of instructive signals such as BMP2 and LIF, they did not differentiate towards astrocytes. BMP2, along with STAT3 activated by LIF, prevents NEUROGENIN expression and subsequently expression of NEUROD1, inhibiting neuronal differentiation. When hNP cells are pre-exposed to the DNMT inhibitor Aza-C, hNP cells become competent for astrocytogenesis upon additional exposure to BMP2 and LIF signaling. This suggests that hES derived hNP cells represent early embryonic neuroepithelial cells in terms of glial potential and epigenetics. The removal of hypermethylation gives a quick and defined way to produce highly enriched astrocytes from hNP cells in a very short time.

Alternatively, Aza-C and TSA may have multiple effects on the hNP cells beyond effecting epigenetic marks on the proastrocytic genes probed. The ability to produce a highly enriched and cryopreservable population of either astrocytes or neurons from the same source will make it possible to co-culture astrocytes and neurons in defined ratios, making it possible to design controlled experiments and assays. Also, this approach eliminates serum commonly used to generate astrocytes increasing the scope of applications for these cells.
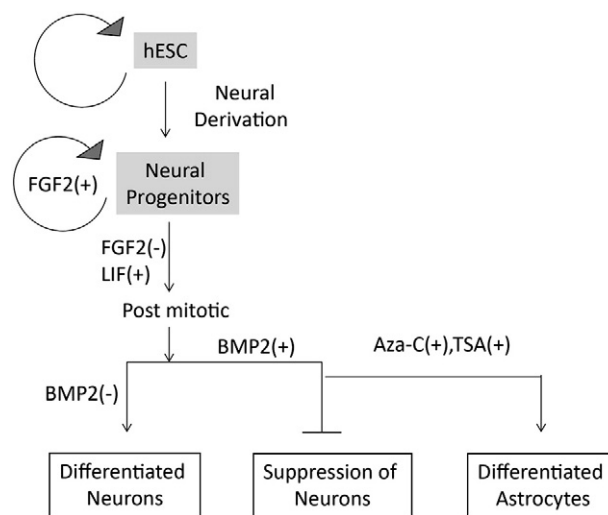

Figure 7 Schematic diagram explaining possible events of astrocyte differentiation with human neural progenitors. Human neural progenitors (hNP) are generated from human ES cells as per described protocol. Presence of FGF2 in culture prevents differentiation of hNP cells into terminal fates such as neurons and glia (astrocytes and oligodendrocytes) and maintains proliferative state, allowing expansion. Withdrawal of FGF2 triggers differentiation and in the absence of any instructive signal, mostly pure neuronal cultures are obtained. BMP2 signaling, which is known to prevent neuronal differentiation, drastically reduces expression of neuronal markers in the differentiated culture. However, BMP2 alone is not sufficient to drive differentiation along the astrocyte lineage. Promoters of pro-astrocytic genes are found to be methylated in hNP cells. Therefore, to overcome this epigenetic blockage, methylation inhibitor Aza-C, in the presence of TSA and another instructive signal, LIF, is used and the cultures become primarily of astrocytic in nature.

Further, this process will allow comparative studies due to early divergence of the two populations and the short time required for appearance of fate specific markers.

Acknowledgments

References

Anthony, T.E., Heintz, N., 2007. The folate metabolic enzyme ALDH1L1 is restricted to the midline of the early CNS, suggesting a role in human neural tube defects. J. Comp. Neurol. 500, 368–383.

Asano, H., Aonuma, M., Sanosaka, T., et al., 2009. Astrocyte differentiation of neural precursor cells is enhanced by retinoic acid through a change in epigenetic modification. Stem Cells 27, 2744–2752.

Balasubramaniyan, V., Boddeke, E., Bakels, R., et al., 2006. Effects of histone deacetylation inhibition on neuronal differentiation of embryonic mouse neural stem cells. Neuroscience 143, 939–951.

Bock, C., Reither, S., Mikeska, T., et al., 2005. BiQ Analyzer: visualization and quality control for DNA methylation data from bisulfite sequencing. Bioinformatics 21, 4067–4068.

Cahoy, J.D., Emery, B., Kaushal, A., et al., 2008. A transcriptome database for astrocytes, neurons, and oligodendrocytes: a new resource for understanding brain development and function. J. Neurosci. 28, 264–278.

Chen, G., Hou, Z., Gulbranson, D.R., et al., 2010. Actin–myosin contractility is responsible for the reduced viability of dissociated human embryonic stem cells. Cell Stem Cell 7, 240–248.

Chireux, M., Espinos, E., Bloch, S., et al., 1996. Histone hyperacetylating agents stimulate promoter activity of human choline acetyltransferase gene in transfection experiment. Brain Res. Mol. Brain Res. 39, 68–78.

Dhara, S.K., Hasneen, K., Machacek, D.W., et al., 2008. Human neural progenitor cells derived from embryonic stem cells in feeder-free cultures. Differentiation 76, 454–464.

Fan, G., Martinowich, K., Chin, M.H., et al., 2005. DNA methylation controls the timing of astrogliogenesis through regulation of JAK–STAT signaling. Development 132, 3345–3356.

Fatemi, S.H., Folsom, T.D., Reutiman, T.J., et al., 2008. Expression of astrocytic markers aquaporin 4 and connexin 43 is altered in brains of subjects with autism. Synapse 62, 501–507.

Freeman, M.R., 2010. Specification and morphogenesis of astrocytes. Science 330, 774–778.

Fu, H., Cai, J., Clevers, H., et al., 2009. A genome-wide screen for spatially restricted expression patterns identifies transcription factors that regulate glial development. J. Neurosci. 29, 11399–11408.

Gage, F.H., Coates, P.W., Palmer, T.D., et al., 1995. Survival and differentiation of adult neuronal progenitor cells transplanted to the adult brain. Proc. Natl. Acad. Sci. U. S. A. 92, 11879–11883.

Gonzalez-Gomez, P., Bello, M.J., Arjona, D., et al., 2003. Promoter hypermethylation of multiple genes in astrocytic gliomas. Int. J. Oncol. 22, 601–608.

Gupta, K., Patani, R., Baxter, P., et al., 2012. Human embryonic stem cell derived astrocytes mediate non-cell-autonomous neuroprotection through endogenous and drug-induced mechanisms. Cell Death Differ. 19, 779–787.

Hatada, I., Namihira, M., Morita, S., et al., 2008. Astrocyte-specific genes are generally demethylated in neural precursor cells prior to astrocytic differentiation. PLoS One 3, e3189.

Hersh, L.B., Shimojo, M., 2003. Regulation of cholinergic gene expression by the neuron restrictive silencer factor/repressor element-1 silencing transcription factor. Life Sci. 72, 2021–2028.

Juttermann, R., Li, E., Jaenisch, R., 1994. Toxicity of 5-aza-2′-deoxycytidine to mammalian cells is mediated primarily by covalent trapping of DNA methyltransferase rather than DNA demethylation. Proc. Natl. Acad. Sci. U. S. A. 91, 11797–11801.

Koblar, S.A., Turnley, A.M., Classon, B.J., et al., 1998. Neural precursor differentiation into astrocytes requires signaling through the leukemia inhibitory factor receptor. Proc. Natl. Acad. Sci. U. S. A. 95, 3178–3181.

Krencik, R., Weick, J.P., Liu, Y., et al., 2011. Specification of transplantable astroglial subtypes from human pluripotent stem cells. Nat. Biotechnol. 29, 528–534.

Liu, Y., Han, S.S., Wu, Y., et al., 2004. CD44 expression identifies astrocyte-restricted precursor cells. Dev. Biol. 276, 31–46.

Majumder, A., Banerjee, S., Harrill, J.A., et al., 2012. Neurotrophic effects of leukemia inhibitory factor on neural cells derived from human embryonic stem cells. Stem Cells 30, 2387–2399.

Mattson, M.P., 2003. Methylation and acetylation in nervous system development and neurodegenerative disorders. Ageing Res. Rev. 2, 329–342.

Matyash, V., Kettenmann, H., 2010. Heterogeneity in astrocyte morphology and physiology. Brain Res. Rev. 63, 2–10.

Molne, M., Studer, L., Tabar, V., et al., 2000. Early cortical precursors do not undergo LIF-mediated astrocytic differentiation. J. Neurosci. Res. 59, 301–311.

Nakashima, K., Yanagisawa, M., Arakawa, H., et al., 1999. Astrocyte differentiation mediated by LIF in cooperation with BMP2. FEBS Lett. 457, 43–46.

Ohgushi, M., Matsumura, M., Eiraku, M., et al., 2010. Molecular pathway and cell state responsible for dissociation-induced apoptosis in human pluripotent stem cells. Cell Stem Cell 7, 225–239.

Sanosaka, T., Namihira, M., Asano, H., et al., 2008. Identification of genes that restrict astrocyte differentiation of midgestational neural precursor cells. Neuroscience 155, 780–788.

Santi, D.V., Norment, A., Garrett, C.E., 1984. Covalent bond formation between a DNA-cytosine methyltransferase and DNA containing 5-azacytosine. Proc. Natl. Acad. Sci. U. S. A. 81, 6993–6997.

Shimozaki, K., Namihira, M., Nakashima, K., et al., 2005. Stage- and site-specific DNA demethylation during neural cell development from embryonic stem cells. J. Neurochem. 93, 432–439.

Shin, S., Mitalipova, M., Noggle, S., et al., 2006. Long-term proliferation of human embryonic stem cell-derived neuroepithelial cells using defined adherent culture conditions. Stem Cells 24, 125–138.

Sofroniew, M.V., Vinters, H.V., 2010. Astrocytes: biology and pathology. Acta Neuropathol. 119, 7–35.

Sun, Y., Nadal-Vicens, M., Misono, S., et al., 2001. Neurogenin promotes neurogenesis and inhibits glial differentiation by independent mechanisms. Cell 104, 365–376.

Takizawa, T., Nakashima, K., Namihira, M., et al., 2001. DNA methylation is a critical cell-intrinsic determinant of astrocyte differentiation in the fetal brain. Dev. Cell 1, 749–758.

Temple, S., 2001. The development of neural stem cells. Nature 414, 112–117.

Wu, Y., Liu, Y., Levine, E.M., et al., 2003. Hes1 but not Hes5 regulates an astrocyte versus oligodendrocyte fate choice in glial restricted precursors. Dev. Dyn. 226, 675–689.

Wu, S.X., Goebbels, S., Nakamura, K., et al., 2005. Pyramidal neurons of upper cortical layers generated by NEX-positive progenitor cells in the subventricular zone. Proc. Natl. Acad. Sci. U. S. A. 102, 17172–17177.

Yan, H., Parsons, D.W., Jin, G., et al., 2009. IDH1 and IDH2 mutations in gliomas. N. Engl. J. Med. 360, 765–773.

Yanagisawa, M., Nakashima, K., Takizawa, T., et al., 2001. Signaling crosstalk underlying synergistic induction of astrocyte differentiation by BMPs and IL-6 family of cytokines. FEBS Lett. 489, 139–143.

Young, A., Machacek, D.W., Dhara, S.K., et al., 2011. Ion channels and ionotropic receptors in human embryonic stem cell derived neural progenitors. Neuroscience 192, 793–805.

Yuan, S.H., Martin, J., Elia, J., et al., 2011. Cell-surface marker signatures for the isolation of neural stem cells, glia and neurons derived from human pluripotent stem cells. PLoS One 6, e17540.

Zhang, Y., Cooke, M., Panjwani, S., et al., 2012. Histone h1 depletion impairs embryonic stem cell differentiation. PLoS Genet. 8, e1002691.